Science of the Total Environment 926 (2024) 172060

Contents lists available at ScienceDirect

Science of the Total Environment

journal homepage: www.elsevier.com/locate/scitotenv

Towards a zero liquid discharge process from brine treatment: Water recovery, nitrate electrochemical elimination and potential valorization of hydrogen and salts

Javier Sanchis-Carbonell [a], Iván Carrero-Ferrer [b], Alfonso Sáez-Fernández [c], María Pedro-Monzonís [a], P. Campíns-Falcó [b,*], Vicente Montiel [c,*]

[a] Aguas de Valencia, S.A., Spain
[b] MINTOTA Research Group, Departament de Química Analítica, Facultat de Química, Universitat de València, Dr. Moliner 50, 46100 Burjassot, València, Spain
[c] Institute of Electrochemistry, Universidad de Alicante, Spain

HIGHLIGHTS

- Zero liquid discharge process of an electrodialysis reversal water treatment plant
- Softening 2000 L of plant brine, demineralizing 500 L of nitrate reduction brine
- Reversed osmosis to recover 75 % of water and enrich the waste (25 %) in nitrate
- Efficient electrochemical reduction of nitrate to nitrogen (60 % in gas current)
- Valorization of subproducts like hydrogen current (97 %) and saline solutions

GRAPHICAL ABSTRACT

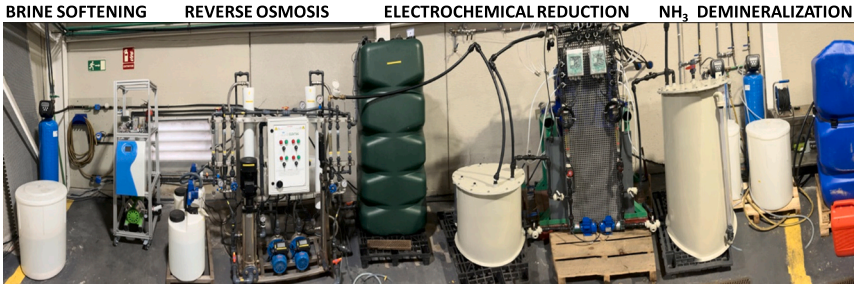

ARTICLE INFO

Editor: Damia Barcelo

Keywords:
Nitrate electrochemical reduction
Ionic exchange
Reverse osmosis
Water cycle
Valorization
Brine treatment

ABSTRACT

This research addresses the issues related with treatment and valorization of brines and nitrate decontamination of surface and ground waters. The objective was to approximate to zero liquid discharge (ZLD) minimizing the environmental impact of brines of an electrodialysis reversal water treatment plant (EDRWTP) as an example. The innovative in flow process was developed from lab to pre-industrial scale and joined several main concepts: ion-exchange equilibrium for softening or demineralization of brines; reversed osmosis to recover suitable water and to enrich the waste in nitrate for efficient electrochemical reduction of NO_3^- to N_2; valorization of subproducts by direct use or by precipitation; and assessment of the whole process by measuring in-line several parameters. The achieved softening was around 98 % and the recovered water from this current by reversed osmosis was 75 %. The brine of this step (25 %) contained around 1500 mg/L of nitrate and it was treated by electrochemical reduction with a Bi/Sn cathode providing a gas current of 60 % of initial nitrate reduced to N_2, O_2, H_2O, NH_3 and at least 97 % of H_2. The aqueous current contained around 40 % of initial nitrate as ammonium and nitrite lower than 50 and 5 mg/L, respectively. Hypochlorite was added to this last current for oxidizing ammonium and nitrite to N_2 and nitrate, respectively, being nitrate and ammonium lower than 50 and 5 mg/L, respectively. After the obtained water was demineralized and conducted to the EDRWTP inlet. The recovery of insoluble salts as calcium carbonate, reuse of saline solutions for the regeneration of process resins

* Corresponding authors.
E-mail addresses: pilar.campins@uv.es (P. Campíns-Falcó), vicente.montiel@ua.es (V. Montiel).

https://doi.org/10.1016/j.scitotenv.2024.172060
Received 14 January 2024; Received in revised form 26 March 2024; Accepted 26 March 2024
Available online 28 March 2024

and the potential use of hydrogen generated as a by-product during the electrochemical reduction are other possible utilities.

1. Introduction

Wastewater generation has increased dramatically as a result of urbanization and industrialization. In particular, those called "brine" or "rejection", come from various facilities, such as water treatment plants, desalination plants, oil and gas production, the pharmaceutical industry. Brine has become a serious environmental problem and a threat to the natural environment. However, the opportunity to recover resources is possible, since the brine is rich in salts. Brines contain in general: sodium, chloride, calcium, potassium, magnesium, nitrate and sulfate ions. In all types, the salinity of these waters can vary between 0.1 and 40 % depending on the source (Panagopoulos, 2022).

On the other hand, excess N in the environment represents globally a serious threat to nature and the climate (Steffen et al., 2015). N is involved in biogeochemical flows as Earth-system process with proposed boundaries and zones of uncertainty established. Planetary boundary (zone of uncertainty) was 62 Tg N yr^{-1} (62–82 Tg N yr^{-1}) and its value was ~150 Tg N yr^{-1} (Steffen et al., 2015). Boundary acts as a global 'valve' limiting introduction of new reactive N to Earth System, but regional distribution of fertilizer N is critical for impacts. Europe contributes considerably to this form of pollution (Joint EEA/FOEN Report, 2020; COM/2021/1000), being agriculture the main cause of the poor chemical status of water bodies due to high nitrate contents (Vinod and Chandramouli, 2015; EEA Report No 7/2018; Vaish et al., 2019; Karlović et al., 2022).

Drinking water with high levels of nitrates over long periods of time can pose different health risk and reproductive problems, according to scientific articles (IARC, 2010; Gao et al., 2020), especially for babies (Apte et al., 2024), having been associated to pathologies such as methemoglobinemia, cancer (Picetti et al., 2022) or disorders of the endocrine system. World Health Organization (WHO, Nitrate and Nitrite Drinking-water, 2003; WHO, Guidelines for drinking-water quality, 2011), European (Directive 91/676/EEC; Directive (EU) 2020/2184) and national legislation in Spain (RD 03/2023), limit the maximum permitted level of nitrates in drinking water to 50 mg/L.

The European directives for the protection of water against pollution caused by nitrates 91/676/EEC, for the protection of water bodies 2000/60/EC, the treatment of waste water 91/271/EEC and on the marine environment 2008/56/EC, have the objective of achieving the "good status" of the water bodies in the EU. The Biodiversity COM/2020b/380, Farm to Fork EU-COM/2020c/381 and European Green Deal COM/2019/640 strategies set the common goal of reducing nutrient losses in the environment by at least 50 % by 2030. Efforts made by Member States to reduce the impact of nitrate pollution should be directed towards achieving climate neutrality by 2050 (COM/2019/640) and using water in a sustainable and efficient form (Gawlik et al., 2017).

As a consequence of the problem generated by the presence of nitrate in water, there has been a growing interest in the development of efficient denitrification technologies. Basically, there are two approaches available in the field of groundwater denitrification: separation techniques and transformation technologies (Abascal et al., 2021).

Separation techniques are based on the displacement of nitrates from the polluted stream to be concentrated in an auxiliary waste stream, including electrodialysis reversal (EDR) (Sharma and Bhattacharya, 2017; Al-Amshawee et al., 2020), nanofiltration (NF) (Santafe-Moros et al., 2005), reverse osmosis (RO) (Sharma and Bhattacharya, 2017), and anion exchange resins (AER) (Sharma and Bhattacharya, 2017), although their main common drawback is the creation of secondary high-nitrate wastewater streams, which should be subsequently managed. The technological solution depends on raw water characteristics, affordability and acceptability and level of application. Of course, sustainability depends on an awareness of the related issues and limitations exist (Sharma and Bhattacharya, 2017).

Transformation techniques are based on the destruction of nitrate by its chemical conversion into other compounds, such us biological denitrification (Sharma and Bhattacharya, 2017), catalytic reduction (Duca and Koper, 2012; Martínez et al., 2017; Sharma and Bhattacharya, 2017; Marchesini et al., 2019; Tokazhanov et al., 2020), and electrocatalytic reduction (Li et al., 2009; Martínez et al., 2017; Garcia-Segura et al., 2018; Gao et al., 2019; Sanjuán et al., 2020; Tokazhanov et al., 2020; Beltrame et al., 2021). Biological processes present limitations due to the formation of sludge and the risk of pathogenic bacterial contamination in drinking water, whereas catalytic technology has no application in industrial environments, in addition to ammonia generating (Pizarro et al., 2018). Electrochemical technology circumvents the drawbacks of previous techniques by reducing nitrate ions to nitrogen, with minimal amounts of other products as demonstrated in patent WO2020128121A1 (Sanjuán et al., 2019, 2020). However, some necessary improvements are necessary: water softening due to the potential precipitation of calcium and magnesium at the cathode, increasing nitrate concentrations (> 500 ppm) to achieve a cost-effective energy consumption and the management of the NH_3 by-product.

There are some works that address the electroreduction of nitrate ions present in waters from the pharmaceutical industry with high saline contents (Peng et al., 2020) to ammonium ions and the simultaneous obtaining of chlorine gas that is later used for the absorption and oxidation of the ammonium ions obtained in the electrochemical reaction. Ma et al., 2020 describes a process for the electrochemical reduction of nitrate ions to ammonium ions using Cu/Zn and Ti cathodes, so that the ammonium obtained is oxidized in the same electrochemical reactor by the hypochlorite that is obtained in the anodic process. Water concentrated by reverse osmosis is simulated, reaching nitrate ion contents close to and below 100 ppm in which the magnesium and calcium ions present in the water precipitate in the electrochemical reactor in the form of hydroxides. Besides there is a propose the reduction of nitrate ions present in different types of water through the use of Sn electrodes, demonstrating that the hardness of the water hinders and minimizes the efficiency of the electrochemical process of reduction of nitrate ions, raising the need to reduce or minimize the hardness of the water (Atrashkevich et al., 2022). In any case, we have not found a global process described that allows the transformation of the nitrate ions present in brines into N_2 inert gas together with obtaining quality water, the recovery of saline ionic compounds and the energy recovery of the current H_2 gas that, however, is obtained in any electrochemical process of reduction of nitrate ions.

The aim of this work is to present an innovative process, with industrial application, designed on a pilot scale based on electrochemical reduction of nitrate ions (REN) with a series of pre- and post-conditioning stages of brine water from the desalination plant, in order to minimize the electrical consumption of the electroreduction stage, to achieve an almost complete transformation of NO_3^- into N_2 with minimal amounts of other products (NH_4^+ or NO_2^-), to regenerate waste streams achieving almost zero liquid discharge (Xiao et al., 2020), and to show the potential valorization of the salts and the H_2 generated as a by-product during the electrochemical reduction of NO_3^-. This process is being evaluated as a patent with application number P202330547 (Montiel et al., 2023) and will be scaled in the LIFE project: Circular economy applied to nitrate removal: hydrogen generation and waste recovery in drinking water LIFE22 ENV/ES/101113771 ELEKTRA.

2. Experimental

2.1. Chemicals and materials

See section S1 of the Supporting information (SI).

Brines of an electrodialysis reversal (EDR) process from a water treatment plant (WTPs) in Gandia (Valencia, Spain) with high nitrate concentration and hardness were assayed. The composition of the reject water from an EDR plant can vary depending on the characteristics of the inlet water and the operating conditions of the plant. However, in general they are characterized by an approximately neutral pH (6.8–7.3) and a conductivity in the range of 3.2 to 4.7 $mScm^{-1}$. Likewise, they present high hardness values, between 220 and 320 °F (Ca^{2+} and Mg^{2+} concentrations higher than 750 mg/L and 250 mg/L, respectively), nitrate concentrations in the range of 320 to 460 mg/L, and sulfates, chlorides, and bicarbonates, mainly sodium, up to 2–3 g/L.

2.2. Instruments

A UV–Vis Spectrophotometer (Cary 60 UV–Vis, Agilent, Santa Clara, CA, USA) and an optical fiber UV–Vis Portable Spectrophotometer (OceanOptics, Orlando, FL, USA) were used. The optical fiber was 300 μm of core and 2 m long and the spectrophotometer was a Maya2000 Pro model. Concerning portable optical fiber probe spectrophotometer the optimized integration time was 50 μs searching a compromise between sensitivity and signal to noise ratio (S/N), the number of scans was 3 and a boxcar smoothing of 5 was selected. The equipment software was used in both cases. To perform the image analysis, pictures were taken with a smartphone using the professional mode of the camera, and the parameters were set to 1–1.3 brightness contrast, ISO100, autofocus mode, and a value of 7077 for color temperature (Martínez-Aviño et al., 2021, 2022). From the images, the intensity in color planes R, G, and B was obtained by the free GIMP program or MINTOTA Spectro-free App (Martínez-Aviño et al., 2021; Monforte-Gómez et al., 2023).

FTIR spectra in the range of 3300–400 cm^{-1} at a resolution of 4 cm^{-1} on a Cary 630 FTIR-ATR spectrophotometer Agilent Technologies was used for identifying recovered $CaCO_3$. For data collection and processing, MicroLab FTIR and Resolution Pro software's (Agilent Technologies) were used, respectively. The softening and demineralization at lab were performed in one or two fixed-bed columns using liquid chromatography columns sigma with a length of 10 cm and 0.75 cm of diameter, which were connected with FIA plastic connections to a peristaltic pump MINIPULS 3 (GILSON, Villiers Le Bel, France). A portable Thermo scientific Orion star A329 (Madrid, Spain) for pH, Na^+ and Cl^- potentiometric measurements and a portable Metrohm 914 for conductimetry and Ca^{2+} potenciometry (Barcelona, Spain) were employed.

A Gas Chromatograph Hitachi 163 GC (Tokyo, Japan) using a thermal conductivity detector was used for analysis of gas phase components (NO_2, NO, N_2O) of electrochemical denitrification tests. The analysis was conducted at constant column temperature of 80 °C and a detector temperature of 250 °C. The chromatographic column was a MS-13× and a pure He stream was the carrier gas. At the same time, a micro gas chromatograph Agilent 990 (Santa Clara, USA) using a column M55A SS 20 Mx0.25MM and pure He as carrier was used for H_2, N_2 and O_2 contents determination in gaseous phase. The analysis of the ions at the liquid phase of the catholyte (NO_3^-, NO_2^- and NH_4^+) was carried out using an ionic Chromatograph Metohm (883 Basic IC plus) (Herisau, CH). NO_3^- and NO_2^- were analyzed using a column metrosep A Supp 4250/4.0 mm with a mobile phase carbonate/bicarbonate and NH_4^+ using a column metrosep C6 250/4.0 mm with a mobile phase nitric acid/dipicolinic acid. $[NO_3^-]_{total}$ was defined as $[NO_3^-]$ plus $[NO_2^-]$ considered as $[NO_3^-]$ expressed in mg/L. "% Produced or remaining substance" was defined as the ratio between N (nitrogen) moles of produced o remaining substance and initial N moles. For pilot process control, a pH meter VWR pH 1100H (Bruchsal, Germany), Conductivity meter VWR CO 3100H (Bruchsal, Germany), Nitrate Spectrophotometer Thermo Scientific AquaMate Plus (Cramlington, England), Calcium and Magnesium meter HANNA HI97752C (Nușfalău, Romania) were used. Nitrite and nitrate were also determined in water matrices by Capillary LC with DAD detection by the method developed in H. R. Robles-Jimarez et al., 2023.

2.3. Procedures

2.3.1. Softening laboratory experiment and valorization of residues

Different experiments were carried out with continuous monitoring of softening using a peristaltic pump, TYGON LMT-55 tubing models SC0021T (Purple-Purple, ID = 2.06 mm) and SC0222T (Black-white, ID = 3, 17 mm) and the Sigma column 10 cm long and 0.75 cm in diameter (10 × 0.75 cm) containing a quantity of exchangers of 0.3 g. A volume of 30 mL of the reject water was processed at a flow rate of 2 mL/min, 5 mL aliquots were collected, and total hardness was determined by titrating these aliquots to pH 10 (NH_3/NH_4^+ buffer) using 0.01 M EDTA and Eriochrome Black T (NET) as indicator. Another experiment was carried out with amounts of around 0.5 g of Amberlite® and zeolite for which 20 mL of treated water were collected and the total hardness was analyzed for both materials.

Starting from prototype I, it contained 0.5 g of Amberlite®/Na^+ in a column (10 × 0.75 cm) and worked at a flow rate of 1.2 mL/min, 30 mL of brine was processed. A volume of 180 mL and 3 g of resin (prototype II) with dimensions of the column (30 × 1.5 cm) and at a flow rate of 11 mL/min was tested. Prototype III contained 50 g of Amberlite® with the dimensions 50 × 3 cm and worked at a flow of 16.8 mL/min, which was the maximum allowed by the peristaltic pump, and 3 L of brine were processed and the total hardness was determined to evaluate softening. Several experiences with 500 mL of brine were carried out with a complete bed of Amberlite® (6 g) in a column (10 × 0.75 cm) at 1.2 mL/min and continuous monitoring of calcium in the composite by a selective calcium electrode. Values for studying the process are taken each 5 mL or 10 mL until reaching 100 mL and between 100 and 500 mL, respectively (see Fig. 1). In some experiments aliquots of 5 mL was taken until 250 mL and of 50 mL between 250 and 500 mL and were measured for stablishing rupture curves. For these aliquots, Ca^{2+}, Na^+ and Cl^- concentrations, pH and conductivity were measured.

For resin regenerating, four experiments were carried out. The first, using a 10 % NaCl regenerating solution, of which the last 25 mL are saved and the first 150 mL are used for salt recovery ($CaCO_3$). The second experiment is carried out with a mixture of 150 mL of the supernatant from the salt recovery from experiment 1, mixed with the last 25 mL that were not used. The two remaining experiments were carried out with 20 % NaCl. Aliquots measurements were made every 5 mL until reaching 175 mL. The measured parameters were: Ca^{2+}, Na^+ and Cl^- concentrations, pH and conductivity. The used prototype was the same that that shown in Fig. 1.

The stablished conditions were scaled in the WTP considering the commercial beds (30 L and 50 L IRC amberlite) and operating in co-flow regeneration: backwash for 9 min at 5 L/min, drawing in down flow brine for 60 min at 2 L/min and rinsing excess brine to drain for 40 min at 5 L/min. For each step the time and the flow rates were optimized. The regeneration of the resin used 12 % NaCl. The brine (2000 L at 320 L/h) of the EDRWTP was passed through the resin and samples were collected at several times for stablishing the adsorption of Ca^{2+} and Mg^{2+}.

2.3.2. Electrochemical denitrification laboratory experiment

The laboratory homemade electrochemical system is shown in Fig. 2. The electrolyte solutions were recirculated by two magnetic pumps Sanso PMD-371 of (Himeji, Japan). The power supply employed was a Elektro Automatik EA-PS 5040-40 A (Viersen, Germany). The homemade electrochemical reactor is shown in Fig. 3. The cathode electrode was a $Bi_{58}Sn_{42}$ plate, and the anode electrode was a DSA plate (a IrO_2 film onto a Ti plate). In both cases with 7 × 9 cm^2 geometric active area. The cationic exchange membrane was a NAFION 450®. Catholyte and

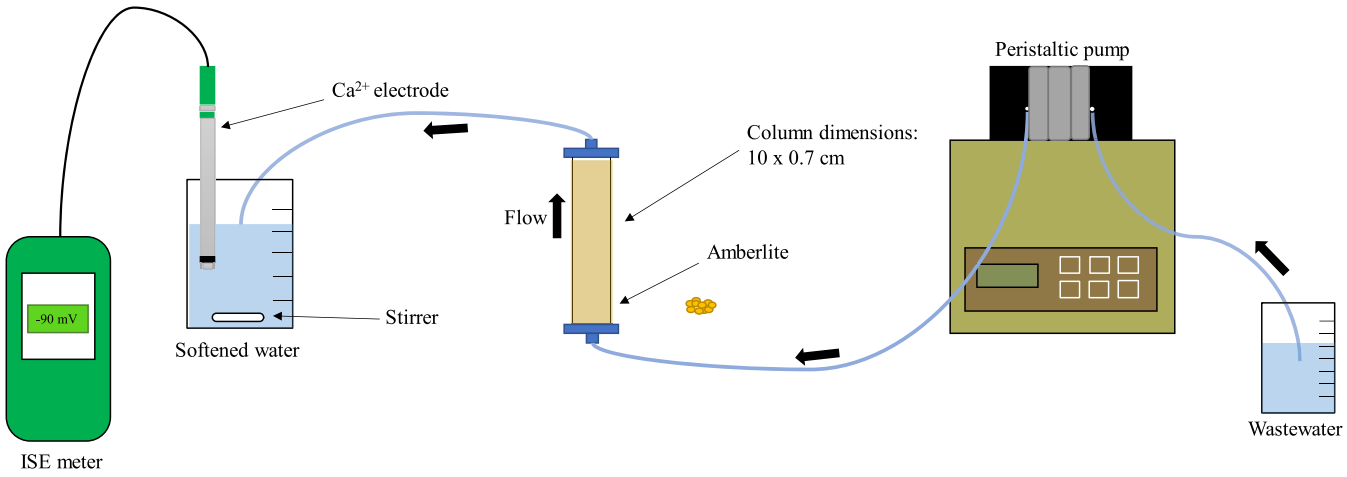

Fig. 1. Lab prototype with complete resin bed and continuous control of Ca^{2+} concentration, pH and conductivity.

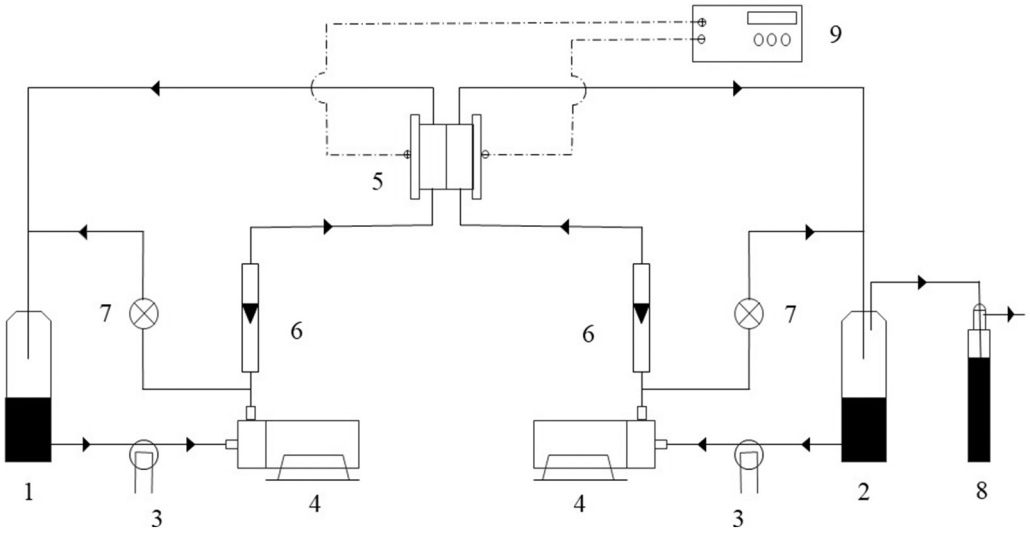

Fig. 2. Laboratory scale electrochemical system: 1. Anolyte vessel. 2. Catholyte vessel. 3. Heat exchanger. 4. Centrifugal pump. 5. Electrochemical reactor. 6. Rotameter. 7. Probe holder (pH, conductivity, temperature). 8. Gas scrubber. 9. Power supply.

anolyte volumes were 0.75 and 1 L, respectively. Catholyte was as well as solution simulating the reject stream from electrodialysis process as the one simulating the same stream at the reverse osmosis process and, anolyte was a H_2SO_4 0.1 M solution. The recirculation flow was fixed at 50 L/h for each compartment. The temperature was controlled at 25 °C. In all experiments the difference of potential between the two electrodes was measured. The gas composition of catholyte line was determined and the NO_3^-, NO_2^- and NH_3 content in the catholyte was measured.

2.3.3. *Integrating other steps*

2.3.3.1. Reverse osmosis. The configuration used was a two-stage reverse osmosis system (Procesos Hidráulicos, Puerto de Sagunto, Spain) with concentrate recirculation in both stages, independent flushing, 5 μm pre-microfiltration, addition of antiscalant (Chemipol WT 810, Terrassa, Barcelona, Spain) and HCl into the feed water. Volumes of 2000 L of EDR softened brine were processed. The membranes used deliver high permeability at low pressure, BW4040ES in the first stage for medium salinity brackish water and BW4040R in the second stage for high salinity brackish water (LG Chem NanoH_2O, Seoul, South Korea). In order to concentrate the nitrate ion, the concentrate recirculation was maximized to 89 % in the first stage and 80 % in the second stage, to reach a nitrate concentration of around 1500 ppm. The 10 bar pressure of the first stage was carried out with a 1.5 kW pump and the 18 bar pressure of the second-stage was carried out with a 2.2 kW pump, an additional tank was used for the accumulation of the first stage concentrate.

2.3.3.2. Gas and water lines of the electrochemical denitrification system. The destruction of the NH_3 present in the catholyte after the electrochemical denitrification process was performed using the breakpoint chlorination process. This process, mainly, converts ammonium to nitrogen gas. Lab scale experiments were carried out in 0,15 L glass beaker equipped with magnetic stirring. Sodium hypochlorite (10 % *w/v*) was added to different solutions with ammonium, nitrate and nitrite-controlled quantities. The concentration of NH_4^+ assayed was between 20 and 300 mg/L and 4 to 20 mg/L for NO_3^- and NO_2^-, respectively. This study was carried out at pH = 8.5, by adding HCl solution (37 % w/v). For each tested solution with the adjusted pH, variable amounts of sodium hypochlorite (10 % w/v) were added and, after one hour of stirring, the contents of NH_4^+, NO_3^- and NO_2^- ions were determined by ion chromatography and the ammonium was also measured by the NQS solid sensor (Campíns-Falcó et al., n.d.). The residual hypochlorite content as free chlorine was measured by iodometric titration

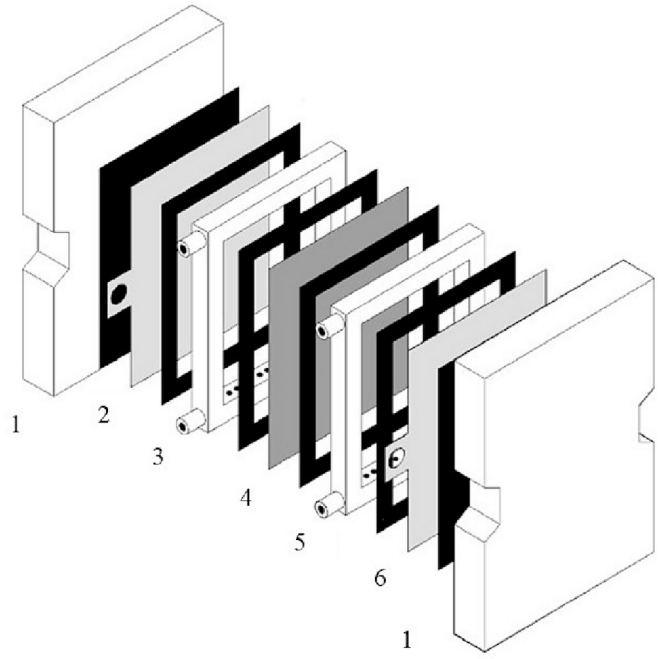

Fig. 3. Filter press type electrochemical reactor. 1. Clamping plate. 2. Anode. 3. Anodic flow distributor. 4. Cationic exchange membrane. 5. Cathodic flow distributor. 6. Cathode. The electrical insulation and sealing elastomer gaskets appear in the in black without numbering.

method. Excess hypochlorite (as total residual chlorine) was eliminated by adding H_2O_2 (3 % *v*/v). The H_2O_2 added concentration was the concentration of free total chlorine (as hypochlorite) multiplied by a factor of 1.1. One hour after the addition of the H_2O_2 solution, aliquots of the final solution were taken, and the total oxidant content was determined by the iodometric titration method and H_2O_2 was determined by the TMB + HRP method (Pla-Tolós et al., 2016).

The gas from the catholyte was washed in a narrow 250 mL gas scrubber bottle containing 50 mL of a 49 g/L sulfuric acid solution. The washed gas was collected in a 250 mL gas bag and H_2, N_2 and O_2 contents were determined using a gas micro-chromatograph. The NH_3 content after gas scrubber bottle was analyzed using the solid sensor (Campíns-Falcó et al., n.d.).

2.3.3.3. Demineralization and valorization of residues. Using the prototype of Fig. 1, Amberlite® IR120 Na^+ (intact or saturated in the softening process) was activated in H^+ form by passing through 36 mL of HCl 12 % and washing with 15 mL of deionized water. In both cases, the recovery of Na^+ or Ca^{2+}, respectively, was studied. The same prototype was used for an anion resin Purofine PFA300 Type II Cl^- for its activation in OH^- form by 40 mL of NaOH 12 % and washing with 15 mL of deionized water and the recovery of Cl^- was monitored. The potential valorization of residues with high contents in Cl^- and Na^+ was studied for activating the amberlite in de Na^+ form. After activation of the two beds, 40 mL of the brine resulting of the nitrate electrodialysis reduction were passed through the amberlite bed and after through purofine bed for demineralization and water recovery.

From the lab studies, the resins were scaled in the WTP, with commercial beds (50 L SSTC60H cation resin and 50 L PFA300 anion resin) with counter-flow regeneration: backwash1 (2 min, 10 L/min), brine (80 min, 1,6 L/min), backwash2 (2 min, 10 L/min) and rinse (5 min, 10 L/min). For each step the time and the flow rates were optimized. The regeneration of the cation resin used 12 % HCl solution and 12 % NaOH for the anion resin. The flow rate (3 L/min) of the previous stage was passed through the double resin and samples were collected for stablishing the absorption of anion and cation, respectively.

After activation of the beds, 50 L of the brine were passed through the two beds as stablished at lab. For all collected aliquots the parameters: Ca^{2+}, Na^+ and Cl^- concentrations, pH and conductivity were measured.

2.3.4. Pilot scale set-up

The pilot-scale was installed in the EDRWTP of Aguas de Valencia in Gandia. A volume of 2000 L of reject water at flow of 320 L/h was passed through 50 L of softening resin containing IRC120 amberlite-Na^+. Volumes of softened brine of 2000 L were concentrated in a double stage reverse osmosis containing a LG BW 4040 ES membrane (5 μm), and 0.4 L/h of 33 % HCl and 0.4 L/h of anti-incrustation (Chemipol WT 810) were dosed. After, 0.32 L of 50 % NaOH were added to adjust pH at 12.8. A batch size of 50 L was taken as a catholyte in a filter press reactor with 1 m^2 of electrode area formed by three elements of 0.33 m^2 ($Bi_{58}Sn_{42}$ cathode, DSA-O2 anode, Nafion® 450 membrane), the anolyte stream was a 0.06 M sulfuric acid solution, the flow rate was maintained at 450 L/h in both anolyte and catholyte, in the experiences carried out in batch. Next, 37 % HCl was added to bring the pH to a value of 8.5 units and 10 % NaClO was dosed to eliminate ammonium. Finally for the demineralization process the obtained last water gone through a double 50 L resin filter, cation resin (Shallow Shell SSTC60H Strong Acid Cation Resin) and anion resin (Purofine PFA300 Type II Strong Base Anion Resin).

3. Results and discussion

The city of Gandia (Valencia, Spain) relies on two EDRWTPs for the purification of the groundwater with brines, which provide a mean composition given in Table 1. Fig. 4 shows a flowchart of the global process, which summarizes the several techniques proposed and the lines of water recovery and brines and the potential use of residues in order to achieve an efficient process near to zero liquid discharge (ZLD). In the following sections the main fundamentals for developing the whole process and the experiments for designing it are described. Finally the good performance of the system is demonstrated bearing in mind the main goal of the research

3.1. Experiments for scaling the whole process

3.1.1. Softening and valorization of residues

The softening achieved using Amberlite® or Zeolite was studied at laboratory (see Section 2.3.1). The total hardness of the untreated rejection water expressed in mg $CaCO_3$/L was 2550 ± 50. The results of these experiments are shown in Fig. S1 of the SI, where it is observed that Amberlite® type resin provided better % softening results than zeolite. Additionally, for the Amberlite® resin in flow performance was better. This resin was selected for further studies.

The scaling of the process in the laboratory maintained the resin mass/rejection water volume ratio and the linear velocity. Starting from prototype I described in Section 2.3.1, the collected volume of 22.5 mL of the treated rejection water presented a softening of about 98 %. A volume of 180 mL of brine and 3 g of resin (prototype II) and 2.25 L and 50 g (prototype III) provided also a softening percentage of 98 %. Fig. 5 shows the softening achieved in prototype III (A) and the experimental breakdown curves for prototype III (B) and two assays at the WTP (C and D) and the models of Thomas (de Franco et al., 2018) and Yan (Radnia et al., 2013) from Eqs. (1) and (2), respectively. From this study it is derived that the scaling is possible, Table 1 shows the results obtained after softening of 2000 L of EDR brine. Table 2 gives the parameters of the applied models. Non-linear fits for these equations were obtained from software SOLVER for Microsoft Excel 2021.

$$\frac{C_t}{C_0} = \frac{1}{1 + exp\left[\frac{K_{Th}}{Q}(q_0 m - C_0 V)\right]} \quad (1)$$

Table 1
Water parameters for the several treatments in the proposed process.

Parameter; units	Input EDR	Brine EDR	Softening	Permeate RO	Brine RO	REN	NH_3 oxidation	De mineralization
Volume; L	20,000	2000	2000	1500	500	500	500	500
Bicarbonate; mg/L	260	1050	1068	214	4282	4252	4158	33
Calcium; mg/L	94	755	<10	0.1	62	<0.5	–	3
Magnesium; mg/L	29	240	<2	0.1	12	<0.5	–	<0.5
Nitrate; mg/L	56	400	420	23.6	1567	9	22	3.5
Hardness; °F		290	<2	–	–	–	–	–
pH	7.6	7.0	7.45	5.4	6.53	8.24	–	11.7
Conductivity 20 °C; μS/cm	680	4000	4267	203	18,280	35,000	34,400	1395
Sodium; mg/L	23	50	1256	107	4704	7307	7619	216
Chloride; mg/L	45.8	593	605	52	2591	2575	7412	72.5
Sulfate; mg/L	83.7	789	805	–	2134	2120	2072	15
Potassium; mg/L	1.3	3.9	–	–	173	–	–	–
Strontium; mg/L	0.35	3.0	–	–	–	–	–	–
Nitrite; mg/L	0.9	–	–	–	–	10	<0.1	<0.1
Ammonium; mg/L	<0.1	–	–	–	–	128	<0.1	<0.1

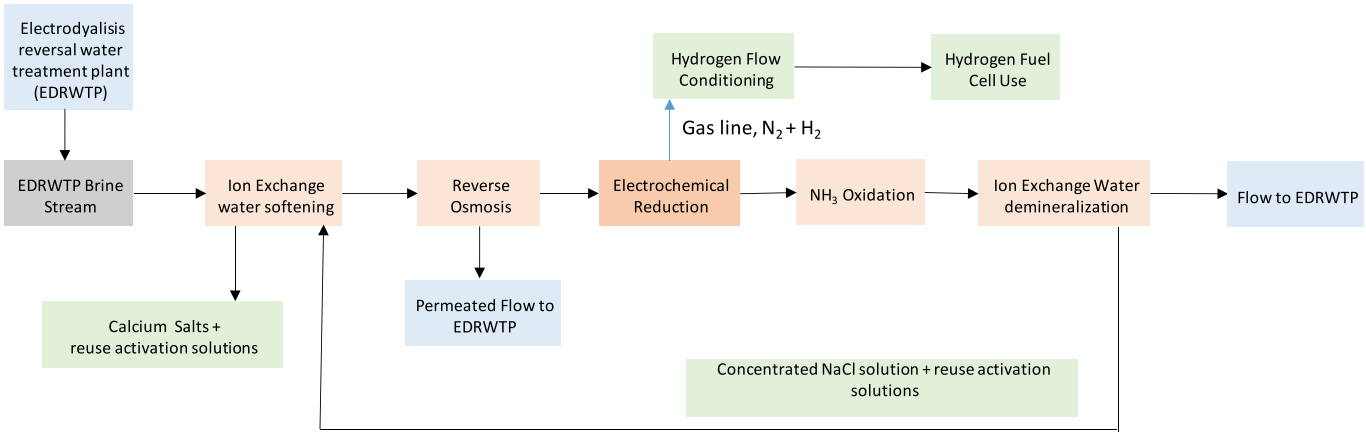

Fig. 4. Flowchart of the proposed process, including techniques, flow inputs and outputs.

where C_t = the effluent concentration (μg/mL), C_0 = the influent concentration (μg/mL), Q = the flow rate (mL/min), V = the effluent volume (mL), m = the mass of the adsorbent (g), t = time (min), kTh is the Thomas rate constant (mL/min mg), q_0 = the maximum adsorption capacity (mg/g)

$$\frac{C_t}{C_0} = 1 - \frac{1}{1 + \left(\frac{QC_0}{q_y m} t\right)^a} \quad (2)$$

where C_0 = the initial solution concentration (μg/mL), Q = the flow rate (mL/min), q_Y = the maximum adsorption capacity (mg/g), m = the amount of adsorbent (g), a = Yan model constant.

The dynamic adsorption is studied by breakthrough curves, which indicates the adsorption concentration in the effluent at the outlet of a fixed-bed adsorbent. According to the coefficient of determinations of Thomas and Yan models shown in Table 2, the adsorption behavior is more in line with the Yan model, which accepts an axial adsorption. The quantity of calcium uptake predicted by this model was Q_y mg/g for the tested brines. The maximum value was obtained for the first use of the resin (50 g) at lab and the activated resin (6 g) with NaCl 20 % provided similar results, lower values were obtained if the activation was carried out with NaCl 10 % (6 g of resin). Similar results were obtained for the softening carried out at WTP, indicating that the step of activation at the plant is similar to the results obtained at lab with 10 % of NaCl.

Fig. 6A and B show the Ca^{2+} and Na^+ punctual concentrations, respectively, obtained by the regenerating of 6 g of exhausted resin with 10 % NaCl and 20 % NaCl (see Section 2.3.1), respectively. It is observed that 20 % NaCl solution provides a greater release of calcium from the resin during regeneration and accordingly the consumption of Na^+ is greater. The softening obtained from the several regenerations are shown in Fig. 6C, which indicates that when more cycles of regenerations are made, better retention capacities are obtained. The composite obtained at 150 mL was employed for recovering the Ca^{2+} ions as carbonate, Fig. 6D gives that the recoveries obtained are 99 % in all cases. These experiences indicate that it is possible to recovery this salt.

3.1.2. Reverse osmosis

A volume of 600 L ($n = 6$) of softened water was circulated through the RO system, the concentrated flow obtained had a value around 1500 mg/L of NO_3^-, and allowed to recover as suitable water >75 % of the softened treated flow, as shown in Table 3. In this way it can be scaled with the aim of limiting the parallel reaction of hydrogen formation in the electrochemical cell. Replicate experiments are shown in Table 3, which gave similar results to those shown in Table 1 for 2000 L of EDR brine softened and treated by RO.

3.1.3. Electrochemical denitrification

The lab scale electrochemical system is described in Section 2.3.2. A synthetic solution simulating the reject stream from reverse osmosis process (expressed in ppm: CO_3^{2-}, 4200; Cl^-, 2100; NO_3^-, 2000; and SO_4^{2-}, 1600; for all salts only Na^+ as cation) as the catholyte was used and a H_2SO_4 0.1 M solution was employed as the anolyte. Values of pH of 9.2, 10.2, 11, and 12.7 were assayed. These values were established wearing in mind the cathode stability. Catholyte and anolyte volumes were 0.75 and 1 L, respectively, and the recirculation flow rate for both was 50 Lh^{-1}. All the experiences were performed at 500 Am^{-2}, with a

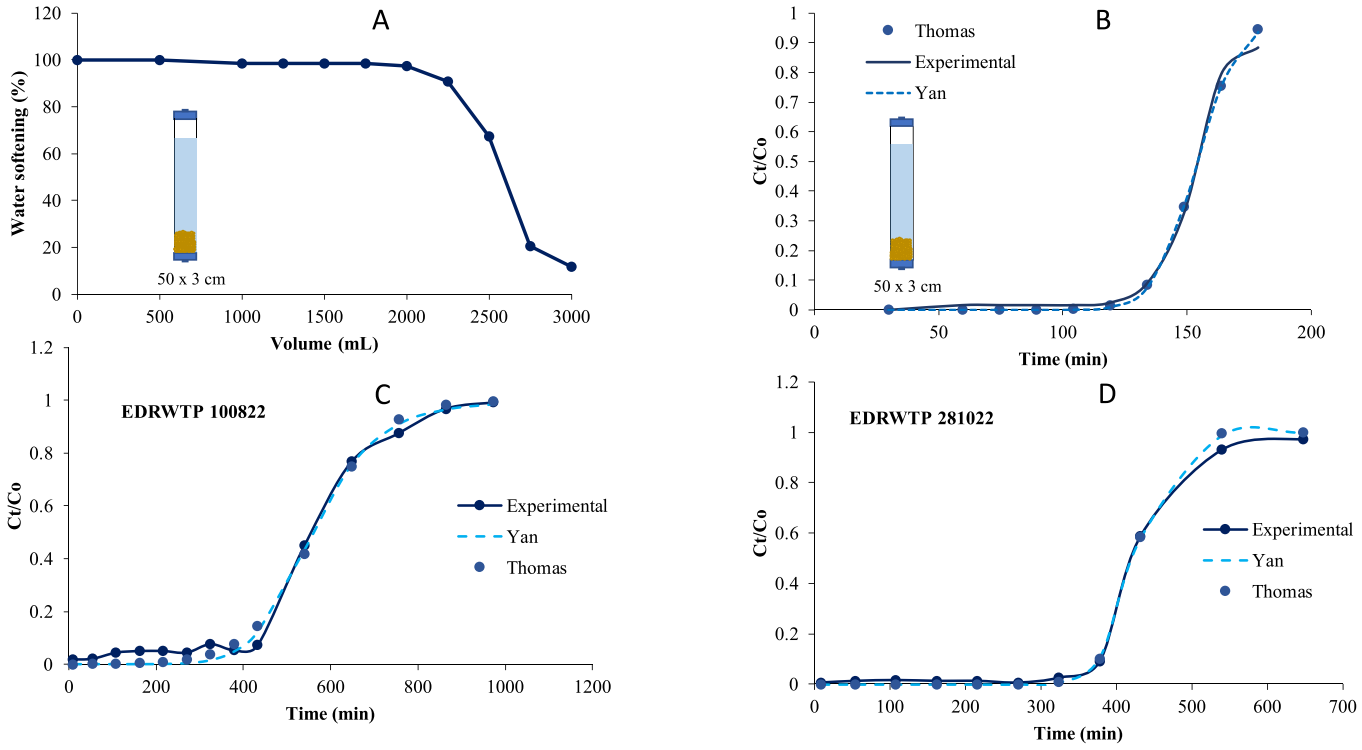

Fig. 5. (A) Softening at lab of the brine in flow with prototype III and (B) its breakdown curve; (C) and (D) breakdown curves of two processes of softening at de EDRWTP.

Table 2
Models of Thomas and Yan for several softening at lab and at WTP.

Resin mass (g)	Thomas model			Yan model		
	K_{th} (mL/h/g)	Q_{th} (mg/g)	R^2	a	Q_y (mg/g)	R^2
50 (lab)	0.0466	130.7446	0.9933	18.0561	130.5428	0.9937
6 (lab)[a]	0.023; 0.023	54.39; 54.34	0.97; 0.98	4.84; 4.71	55.41; 55.54	0.99; 0.99
6 (lab)[b]	0.022; 0.022	98.06; 98.06	0.89; 0.89	7.11; 6.17	107.82; 118.17	0.90; 0.90
30,000 (WTP)	0.0241	57.7742	0.9906	7.6488	57.1495	0.9910
30,000 (WTP)	0.0953	38.5094	0.9960	18.3345	38.4840	0.9964

[a] Activated resins with NaCl 10 %.
[b] Activated resins with NaCl 20 %.

charge circulated of 37.8 or 44 Ah L^{-1}. Fig. 7 shows the values of $[NO_3^-]_{total}$ versus charge circulated for each initial pH. The efficiency was the greatest in the process carried out at pH =12.7 as Fig. 7 shows.

At pH = 12.7, concentration values of species in liquid phase such as $[NO_3^-]$, $[NO_3^-]_{total}$, $[NO_2^-]$, and $[NH_4^+]$ are depicted versus charge circulated in Fig. S2A of the SI. $[NO_3^-]$ and $[NO_3^-]_{total}$ (see Section 2.2) had a decreasing profile and $[NO_2^-]$ a maximum value of around 200 mg/L at, approximately, 15 Ah L^{-1} and, after that, $[NO_2^-]$ diminished. A constant final value of $[NH_4^+]$ was also observed. Fig. S2B shows the parameter "% of the nitrogen based-species" defined in Section 2.2 for each tested value of charge circulated. These nitrogen based-species are NO_3^-, NO_2^-, NH_4^+ and volatile species (named as "gases"), mainly N_2 (Sanjuán et al., 2020). At the end of the process nitrate was removed and ammonia and nitrogen gas in a ratio around 40/60 was obtained. Finally, it was highlighted, the stability of the pH and the cell potential difference along the experiences (Fig. S2C).

The electrochemical denitrification process was satisfactory by maintaining a pH of the catholyte above 9, with better results being obtained at 12.7. A current density value of 500 A/m^2 was appropriated to establish the conditions for subsequent scaling to the pilot stage.

3.1.4. NH_3 oxidation

The water from the electrochemical reduction cell at pH = 12.7 contained NH_3. Synthetic solutions equivalent to the effluents obtained after the electrochemical denitrification process were considered, adjusting their pH to 8.5 by adding 33 % HCl and considering NH_4^+ concentrations in solutions of 300, 100, 60 and 20 ppm. The breaking point in the NH_4^+ elimination process through chlorination using NaClO was determined at lab scale. A commercial NaClO solution was used as a chlorinating agent for an hour, the concentration of which was determined by iodimetry. For normalization and comparison of results a relationship was considered: $[NaClO]_{stoichiometric} = 1.5\ [NH_4^+]_{initial}$ and dosage of NaClO was established based on $[NaClO]_{stoichiometric}$. The remaining total chlorine concentration expressed as a function of $[NaClO]_{stoichiometric}$ was determined by iodimetry for the different NH_4^+ concentrations and the NaClO dosages carried out (Fig. S3). As Fig. S3 shows for the breaking point, total chlorine in solution was around 0.2 $[NaClO]_{stoichiometric}$. Values of $[NO_3^-]$, $[NO_2^-]$ and $[NH_4^+]$ initials and at the breakpoint for each experience are given in Table 4.

Hydrogen peroxide was used as a dechlorinator agent and 1.1 times of stoichiometric addition of H_2O_2 3 % *v*/v (dilution 1/10 of commercial H_2O_2 30 % *v*/v) produced the elimination of oxidants in the solution with the same values of $[NO_3^-]$ and $[NO_2^-]$. A slight excess of 4 ppm of H_2O_2 was detected using the TMB-HRP method (Pla-Tolós et al., 2016).

3.1.5. Catholyte gas stream

Regarding the catholyte gas stream (see Fig. 4), N-based gas species and oxygen gas crossover from the anolyte compartment were determined. First, NH_3 removal from the gas phase was performed using a trap containing a 0.5 M H_2SO_4 solution. The amount of NH_4^+ obtained was lower than 0.5 mg/L (Campíns-Falcó et al., n.d. sensor). At this point, samples of this catholyte gas stream were collected in gas bags. On

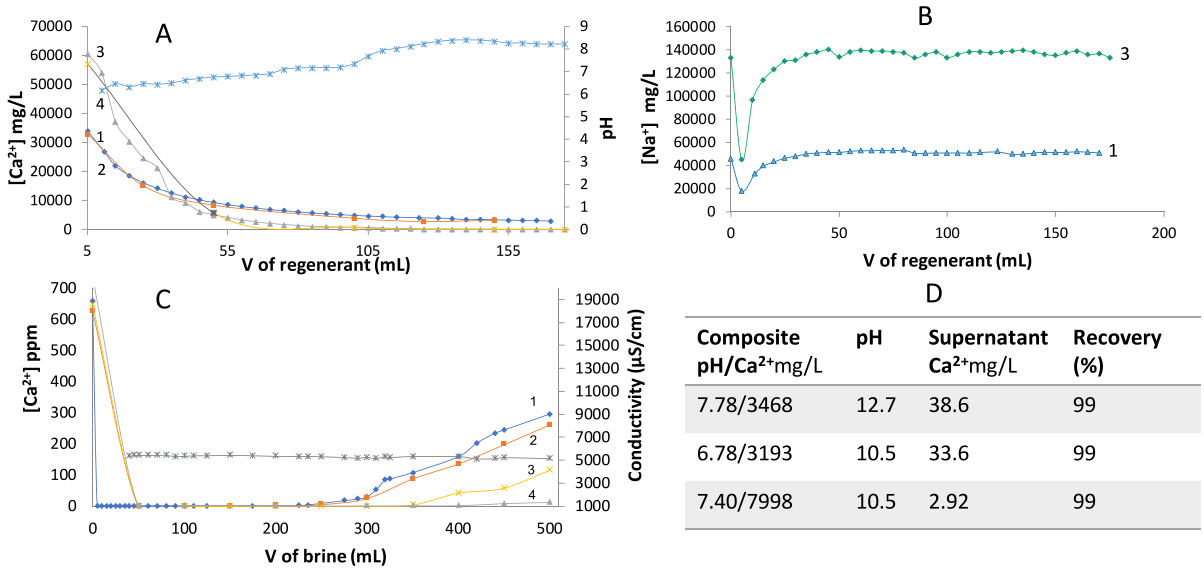

Composite pH/Ca^{2+}mg/L	pH	Supernatant Ca^{2+}mg/L	Recovery (%)
7.78/3468	12.7	38.6	99
6.78/3193	10.5	33.6	99
7.40/7998	10.5	2.92	99

Fig. 6. A) Punctual concentrations of Ca^{2+} obtained for several regenerations of exhausted resin in function of processed volume: 1 (blue) and 2 (orange) with NaCl 10 % and 3 (yellow) and 4 (gray) with NaCl 20 % and pH measurements and B) punctual concentrations of Na^{+} for 1 (blue) and 3 (green) regenerations. C) Composite concentrations of Ca^{2+} for brine softening by using the regenerated resin 1, 2, 3, and 4 and measured conductivity. D) Recoveries of $CaCO_3$ from the first 150 mL of the composite corresponding to the softening carried out with the regenerations 1, 2 and 3.

Table 3
Nitrate concentration and conductivity obtained by softening and RO of 600 L of EDR brine and percentage of water recovered as permeate.

Date	Softening		Permeate			Concentrate	
	Conductivity 20 °C (µS/cm)	Nitrate mg/L	Conductivity 20 °C (µS/cm)	Nitrate mg/L	% recovered volume	Conductivity 20 °C (µS/cm)	Nitrate mg/L
10/08/2023	5610	490	323	38	77	13,110	1133
11/08/2023	5450	468	484	88	76	18,470	1660
14/08/2023	6460	488	551	93	74	18,850	1475
17/08/2023	6010	433	456	94	76	18,400	1532
29/08/2023	5000	459	387	68	81	15,810	1373
31/08/2023	4940	451	414	82	78	18,290	1594

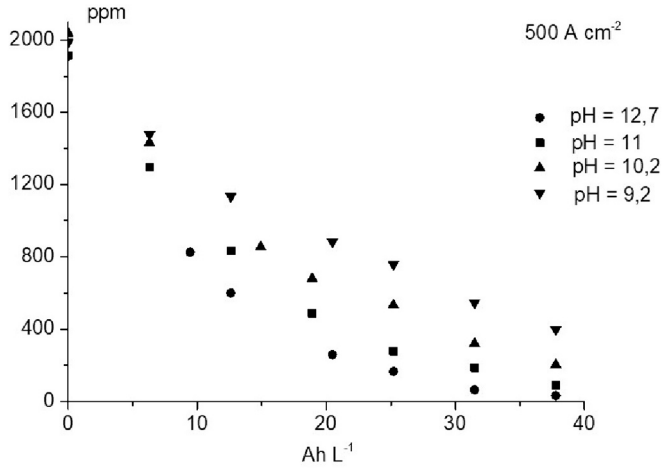

Fig. 7. Electrochemical denitrification for synthetic solutions simulating reject stream from reverse osmosis process. Curves of $[NO_3^-]_{total}$ versus charge circulated for pH of 9.2, 10.2, 11 and 12.7. Current density: 500 A m^{-2}. Recirculating flow rate: 50 L h^{-1}.

Table 4
Initials and breakpoint chlorination values of $[NO_3^-]$, $[NO_2^-]$ and $[NH_4^+]$ expressed in ppm.

Initial			Breakpoint chlorination		
NH_4^+	NO_3^-	NO_2^-	NH_4^+	NO_3^-	NO_2^-
280	20	20	<0.1	35	12
111	19	21	<0.1	39	12
70	5	5	<0.1	14	2
22	4	4	<0.1	6	2

the one hand, no presence of NO, N_2O and, NO_2 in the gas phase was corroborated by gas chromatography analysis (Section 2.2) and, on the other hand, N_2, O_2 and, H_2 was determined using a micro gas chromatograph (Section 2.2.). Considering N_2 as the unique N-based specie at the gas phase and the air presence at the samples because of the residual presence at the electrochemical system, the composition of the catholyte gas stream is evaluated as: H_2 94%, N_2 2%, O_2 1% and H_2O 3 % (wet gas production). A hydrogen stream with an estimated final composition of H_2 (97.9 %) and N_2 (2.1 %) was obtained, which is useful to power a fuel cell and be able to obtain electrical energy to reduce the energy cost of the electrodenitrification process. Concentration of the

several ions for the several steps of the flow process (Fig. 4) are given in Table 1.

3.1.6. Demineralization and valorization of residues

A post-treatment step of demineralization was developed at lab (see Section 2.3.3.3). The best option was: to pass the water obtained from NH_3 oxidation (see Fig. 4) through the amberlite activated as H^+ and the resulting water through the purefine activated as OH^- and without any waste. Fig. 8A shows the results obtained by activating with HCl 12 % amberlite and Fig. 8B the achieved retention of Na^+. Fig. 8C and D give the results for activation of purefine with NaOH 12 % and the retention of Cl^-, respectively. The obtained breakdown curves and the models of Thomas (de Franco et al., 2018) and Yan (Radnia et al., 2013) from Eqs. (1) and (2), respectively are given in Fig. 9. The scaling of the process in the WTP provided similar results for the several concentrations measured as it is given in Table 1.

The obtained demineralization stream can be conveniently integrated in the whole system (see Table 1 and Fig. 4). The regeneration waters of the cationic and anionic resins (as H^+ and OH^-, respectively) for the demineralization process can be useful for regeneration of amberlite resin in the form of Na^+ used in the softening stage.

3.2. Pre-industrial set-up

The flowchart of the pilot is in Fig. 4. First, the water with the composition given in Table 1 is circulated through the softening filter obtaining the breakdown curves of Fig. 6 with their parameters given in Table 2 and the water composition given in Table 1. Secondly the RO concentrates the nitrates up to the value of about 1500 mg/L as shown in Section 3.1.2. Thirdly, the scaling up of the electrochemical denitrification step was verified by the performance of several experiments in the electrochemical reactor. Three tests have been carried out, with reference 300523B, 010623 A and 010623B, with a current density of 500 A/m^2, passing an intensity of 165 A, with a total circulated charge of 30 AhL^{-1}.The analytical and electrical data from the three tests are shown in Tables 5–7, respectively.

The next step in accordance with Fig. 4 is the NH_3 oxidation step. Then, conditioning of pilot plant batches were carried out, adding NaClO and H_2O_2, as Table 8 indicates.

Finally, the water with a conductivity of 34,400 μS/cm is demineralized by exchange resins as indicated above at a flow rate of 3 L/min, obtaining 105 L of water with a conductivity of 1395 μS/cm, proceeding to regenerate the resin to continue the process. Composition of the water are shown in Table 1 and in accordance with the obtained values, this water flow can be conducted to EDRWTP as Fig. 4 indicates.

Additionally, the H_2 gas stream of 1.3 L/min with a temperature of 65 °C obtained from the catholyte line, once purified and pressurized for storage via hydrides, feeds the fuel cell at a density current of 136 mA/cm^2, obtaining a charge of 69 Ah, demonstrating the concept that the gas current obtained in the denitrification process can be valorized.

The energy consumption of the process was concentrated for one part at the high pressure osmosis pumps with the flushing and the dosing pumps, with a consumption of 0.378 kWh to produce the 50 L of concentrate to treat for 150 min in batch in the electrochemical cell, with an intensity of 165 A, which requires a consumption of 6.825 kWh.

4. Conclusions

This study focuses on brine treatment and valorization, as well as nitrate pollution of surface and groundwater. This work has allowed the creation of an innovative, sustainable and transferable process based on the use of ion exchange resins, reverse osmosis technology and electrochemical denitrification to eliminate nitrate towards its conversion into nitrogen gas. The obtained water was demineralized and conducted to the EDRWTP inlet. The recovery of calcium carbonate, reuse of saline solutions for the regeneration of process resins and the potential use of hydrogen generated as a by-product are also possible.

This is a new approach to brine treatment with concentrations of 400 mg/L NO_3^- and hardness of 290 °F, to obtain quality water suitable for reuse with conductivities around 500 μS/cm. A zero liquid discharge process can be achieved, which prevents the effects of pollution in water bodies, ensuring the correct supply of water in quantity and quality and taking advantage of a renewable resource for the generation of clean energy.

The demonstration of the prototype has been carried out at the Gandia reversible electrodialysis plant (TRL7) and will allow the results to be transferred to municipalities that have the same problem of high nitrate concentrations, contributing to the transition towards an efficient economy in the use of resources, protection and improvement of the quality of the environment. More work is being carried out to scale the industrial prototype in the context of the LIFE project: Circular economy applied to nitrate removal: hydrogen generation and waste

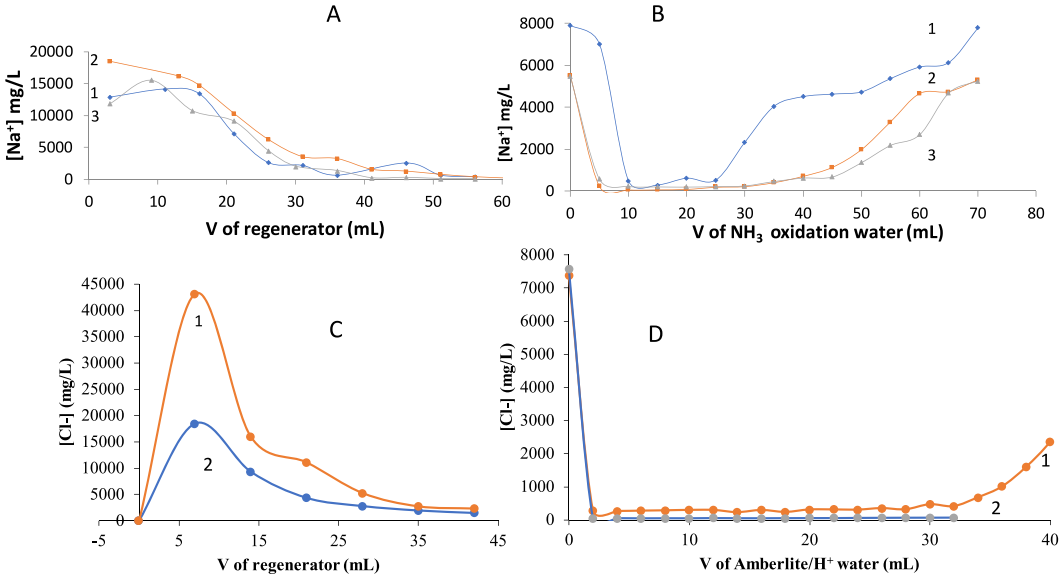

Fig. 8. Three activations (1, 2, 3) of amberlite with HCl 12 % (A) and the results of the treatment of the water obtained from NH_3 oxidation (1, 2, 3) by this resin (B). Two activations (1, 2) of purofine with NaOH 12 % (C) and the results of the treatment (1, 2) of the water obtained from amberlite by purofine (D).

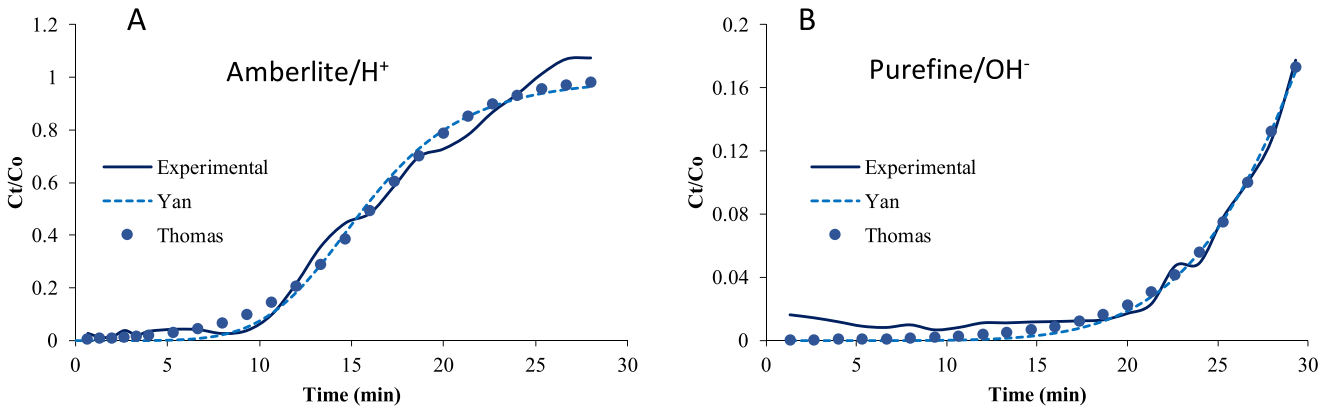

C

Resin mass (g)	Thomas model K_{th} (mL/h/g)	Thomas model Q_{th} (mg/g)	Thomas model R^2	Yan model a	Yan model Q_y (mg/g)	Yan model R^2
6 (lab) Amberlite/H^+	0.0474	44.83	0.972	6.20	47.18	0.964
6 (lab) Amberlite/H^+	0.203	48.15	0.992	9.16	47.86	0.989
6 (lab) Amberlite/H^+	0.190	52.36	0.975	9.37	52.09	0.949
6 (lab) Purefine/OH^-	0.0447	29.673	0.987	5.608	28.928	0.982

Fig. 9. Breakdown curves for amberlite (A) and purofine (B) and models of Thomas and Yan and their parameters (C).

Table 5
Analytical and electrical results for batch 300523B: $pH_{initial} = 12.7$ and $pH_{final} = 12.8$; $\sigma_{initial} = 28.9$ mS cm^{-1} and $\sigma_{final} = 31.7$ mS cm^{-1}. For more explanations see text.

Analytical values				
Ah L^{-1}	NO_3^-/ppm	NO_2^-/ppm	NO_{3total}^-/ppm	NH_4^+/ppm
0	1360	<0.1	1360	<0.1
4.12	1010	21	1040	86
8.23	640	28	690	153
12.35	330	28	370	201
18.94	100	16	130	245
23.05	49	9	63	–
26.35	13	6	22	–
29.64	13	3.5	18	258

Electrical values					
Ah L^{-1}	$\Delta E_{reactor}$/V	ΔE1/V	ΔE2/V	ΔE3/V	I/A
0	17.7	6.4	5.3	5.7	165
4.12	16.8	5.1	5.1	5.4	165
8.23	16.2	5.8	5.0	5.2	165
12.35	15.8	5.6	4.8	5.0	165
18.94	15.3	5.4	4.6	4.9	165
23.05	15.2	5.4	4.6	4.9	165
26.35	15.2	5.4	4.6	4.9	165
29.64	15.1	5.4	4.6	4.8	165

Table 6
Analytical and electrical results for batch 010623A: pH $_{initial} = 12.7$ and $pH_{final} = 12.8$; $\sigma_{initial} = 28.9$ mS cm^{-1} and $\sigma_{final} = 31.7$ mS cm^{-1}. For more explanations see text.

Analytical values				
Ah L^{-1}	NO_3^-/ppm	NO_2^-/ppm	NO_{3total}^-/ppm	NH_4^+/ppm
0	1530	<0.1	1530	<0.1
4.09	1040	28	1080	80
8.18	690	31	740	146
12.28	380	28	420	193
17.19	170	22	200	235
24.55	53	9	65	262
29.46	20	2	23	266

Electrical values					
Ah L^{-1}	$\Delta E_{reactor}$/V	ΔE1/V	ΔE2/V	ΔE3/V	I/A
0	17.1	6.2	5.2	5.4	165
4.09	16.5	5.9	5.0	5.3	165
8.18	16.1	5.8	4.9	5.1	165
12.28	15.5	5.6	4.7	5.0	165
17.19	15.3	5.5	4.6	4.9	165
24.55	15.1	5.4	4.6	4.8	165
29.46	15.0	5.4	4.5	4.8	165

recovery in drinking water LIFE22 ENV/ES/101113771 ELEKTRA.

CRediT authorship contribution statement

Javier Sanchis-Carbonell: Writing – review & editing, Writing – original draft, Investigation, Funding acquisition, Conceptualization. **Iván Carrero-Ferrer:** Validation, Methodology, Investigation. **Alfonso Sáez-Fernández:** Writing – review & editing, Methodology, Conceptualization. **María Pedro-Monzonís:** Writing – review & editing, Methodology. **P. Campíns-Falcó:** Writing – review & editing, Supervision, Methodology, Investigation, Funding acquisition, Conceptualization. **Vicente Montiel:** Writing – review & editing, Resources, Investigation, Funding acquisition, Conceptualization.

Declaration of competing interest

The authors declare that they have no known competing financial interests or personal relationships that could have appeared to influence the work reported in this paper no conflict of interest.

Table 7
Analytical and electrical results for bacth 010623B: $pH_{initial} = 12.7$ and $pH_{final} = 12.8$; $\sigma_{initial} = 28.9$ mS cm^{-1} and $\sigma_{final} = 31.7$ mS cm^{-1}. For more explanations see text.

Analytical values				
Ah L^{-1}	NO_3^-/ppm	NO_2^-/ppm	NO_{3total}^-/ppm	NH_4^+/ppm
0	1390	<0.1	1390	<0.1
4.15	930	31	980	82
8.308	610	41	670	142
12.46	340	57	430	188
16.61	90	32	140	243
23.26	45	15	67	256
29.91	23	2	26	258

Electrical values					
Ah L^{-1}	$\Delta E_{reactor}$/V	ΔE1/V	ΔE2/V	ΔE3/V	I/A
0	17.3	6.4	5.3	5.5	165
4.15	16.4	6.1	5.1	5.3	165
8.308	15.8	5.8	4.9	5.1	165
12.46	15.8	5.8	4.9	5.1	165
16.61	15.2	5.6	4.7	4.9	165
23.26	15.0	5.5	4.6	4.9	165
29.91	14.8	5.4	4.5	4.8	165

Table 8
Added amounts of reagents for ammonia oxidation and determined concentrations of nitrogen containing ions.

Batch	NaClO 1.125 M	H_2O_2 9.354 M	NO_3^-/ ppm	NO_2^-/ ppm	NH_4^+/ ppm	pH
300523B	1440 mL	69 mL	34 ± 3	<0.1	<0.1	8.02
010623A	1490 mL	54 mL	58 ± 3	<0.1	<0.1	8.16
010623B	1450 mL	37 mL	61 ± 3	<0.1	<0.1	7.85

Data availability

Data will be made available on request.

Acknowledgments

Authors acknowledge to the Agencia Valenciana de la Innovación-GV (INNEST/2021/20) and EU (Programme for Environment and Climate Action LIFE) 101113771 LIFE22-ENV-ES-LIFE ELEKTRA for financial support. I. C.-F. thanks to the Generalitat Valenciana-EU for his predoctoral grant CIACIF/2021/079.

Appendix A. Supplementary data

Supplementary data to this article can be found online at https://doi.org/10.1016/j.scitotenv.2024.172060.

References

Abascal, E., Gómez-Coma, L., Ortiz, I., Ortiz, A., 2021. Global diagnosis of nitrate pollution in groundwater and review of removal technologies: a review. Sci. Total Environ. 2022, 152233.
Al-Amshawee, S., Bin Mohd Yunus, M.Y., Mohd Azoddein, A.A., Hassell, D.G., Dakhil, I. H., Hasan, H.A., 2020. Electrodialysis desalination for water and wastewater: a review. Chem. Eng. J. 380, 122231.
Apte, M., Nadavade, N., Sheikh, S.S., 2024. A review on nitrates' health benefits and disease prevention. Nitric Oxide 142, 1–15.
Atrashkevich, A., Fajardo, A.S., Westerhoff, P., Walker, W.S., Sánchez-Sánchez, C.M., Garcia-Segura, S., 2022. Overcoming barriers for nitrate electrochemical reduction: by-passing water hardness. Water Res. 225, 119118.
Beltrame, T.F., Zoppas, F.M., Gomes, M.C., Ferreira, J.Z., Marchesini, F.A., Bernardes, A. M., 2021. Electrochemical nitrate reduction of brines: improving selectivity to N2 by the use of Pd/activated carbon fiber catalyst. Chemosphere 279, 130832.
Campíns-Falcó, P., Moliner-Martínez, Y., Herráez-Hernández, R., Verdú-Andrés, J.; Jornet-Matínez, N. Device for the detection and/or determination in situ of amines and ammonia. Patents ES 2 619 356 B1, ES 2 519 891 A1, EP 3 001 184 B1.
COM/2019/640 final. Communication from the Commission – The European Green Deal.
COM/2020/380 final. Communication from the Commission – EU Biodiversity Strategy for 2030 – Bringing natura back into our lives.
COM/2020/381 final communication from the Commission – A Farm to Fork Strategy for a fair, healthy and environmentally-friendly food system.
COM/2021/1000 final. Report from the Commission to the Council and the European Parliament on the implementation of Council Directive 91/676/EEC concerning the protection of waters against pollution caused by nitrates from agricultural sources based on Member State reports for the period 2016–2019.
De Franco, M.A.E., De Carvalho, C.B., Bonetto, M.M., De Pelegrini Soares, R., Féris, L.A., 2018. Diclofenac removal from water by adsorption using activated carbon in batch mode and fixed-bed column: isotherms, thermodynamic study and breakthrough curves modeling. J. Clean. Prod. 181, 145–154.
Directive 2000/60/EC of the European Parliament and of the Council of 23 October 2000 establishing a framework for Community action in the field of water policy.
Directive 2008/56/EC of the European Parliament and of the Council of 17 June 2008 establishing a framework for community action in the field of marine environmental policy.
Directive (91/271/EEC). Council Directive of 21 May 1991 concerning urban waste water treatment.
Directive (91/676/EEC). Council directive of 12 December 1991 concerning the protection of waters against pollution caused by nitrates from agricultural sources.
Directive (EU) 2020/2184 of the European Parliament and of the Council of 16 December 2020 on the quality of water intended for human consumption.
Duca, M., Koper, M.T.M., 2012. Powering denitrification: the perspectives of electrocatalytic nitrate reduction. Energy Environ. Sci. 5, 9726–9742.
EEA Report No 7/2018, 2018. European Waters. Assessment of Status and Pressures 2018, ISBN 978-92-9213-947-6.
Gao, W., Gao, L., Shen, X., Li, D., Liang, J., Guan, Y., Cui, L., Meng, J., 2019. Preparation of a novel Cu-Sn-Bi cathode and performance on nitrate electroreduction. Water Sci. Technol. 79, 198–206.
Gao, S., Li, C., Jia, C., Zhang, H., Guan, Q., Wu, X., Wang, J., Lv, M., 2020. Health risk assessment of groundwater nitrate contamination: a case study of a typical karst hydrogeological unit in East China. Environ. Sci. Pollut. Res. Int. 27, 9274–9287.
Garcia-Segura, S., Lanzarini-Lopes, M., Hristovski, K., Westerhoff, P., 2018. Electrocatalytic reduction of nitrate: fundamentals to full-scale water treatment applications. Appl. Catal. B Environ. 236, 546–568.
Gawlik, B.M., Easton, P., Koop, S., Van Leeuwen, K., Elelman, R. (Eds.), 2017. Urban Water Atlas for Europe. European Commission, Publications Office of the European Union, Luxembourg.
International Agency for Research on Cancer (IARC), 2010. World health organization international agency for research on cancer, Iarc Monogr. Eval. Carcinog. Risks To Humans 94, 1–464.
Joint EEA/FOEN Report, 2020. Is Europe Living Within the Limits of Our Planet? An Assessment of Europe's Environmental Footprints in Relation to Planetary Boundaries.
Karlović, I., Posavec, K., Larva, O., Marković, T., 2022. Numerical groundwater flow and nitrate transport assessment in alluvial aquifer of Varaždin region, NW Croatia. J. Hydrol. Reg. Stud. 41, 101084.
Li, M., Feng, C., Zhang, Z., Sugiura, N., 2009. Efficient electrochemical reduction of nitrate to nitrogen using Ti/IrO2–Pt anode and different cathodes. Electrochim. Acta 54, 4600–4606.
Ma, X., Li, M., Feng, C., He, Z., 2020. Electrochemical nitrate removal with simultaneous magnesium recovery from a mimicked RO brine assisted by in situ chloride ions. J. Hazard. Mater. 388, 122085.
Marchesini, F.A., Mendow, G., Picard, N.P., Zoppas, F.M., Aghemo, V.S., Gutierrez, L.B., Querini, C.A., Miró, E.E., 2019. PdIn catalysts in a continuous fixed bed reactor for the nitrate removal from groundwater. Int. J. Chem. React. Eng. 17, 20180126.
Martínez, J., Ortiz, A., Ortiz, I., 2017. State-of-the-art and perspectives of the catalytic and electrocatalytic reduction of aqueous nitrates. Appl Catal B 207, 42–59.
Martínez-Aviño, A., Molins-Legua, C., Campíns-Falcó, P., 2021. Scaling the analytical information given by several types of colorimetric and spectroscopic instruments including smartphones: rules for their use and establishing figures of merit of solid chemosensors. Anal. Chem. 93, 6043–6052.
Martínez-Aviño, A., de Diego-Llorente-Luque, M., Molins-Legua, C., Campíns-Falcó, P., 2022. Advances in the measurement of polymeric colorimetric sensors using portable instrumentation: testing the light influence. Polymers 14, 4285.
Monforte-Gómez, B., Hakobyan, L., Molins-Legua, C., Campíns-Falcó, P., 2023. Passive solid chemosensor as saliva point of need analysis for ammonium determination by using a smartphone. Chemosensors 11, 387.
Montiel, V., Expósito, E., Sáez, A., Campins-Falcó, P., Molins-Legua, C., Carrero-Ferrer, I., Sanchis-Carbonell, J., 2023. Procedimiento para la recuperación de agua y eliminación de iones nitrato en corrientes acuosas salinas y equipo para llevar a cabo dicho procedimiento (Spain, Patent Application P202330547).
Panagopoulos, A., 2022. Study and evaluation of the characteristics of saline wastewater (brine) produced by desalination and industrial plants. Environ. Sci. Pollut. Res. 29, 23736–23749.
Peng, P., Hongfei, Z., Le, Z., 2020. CN110803812 Method and System for Treating High-salt and High-nitrate Industrial Wastewater.
Picetti, R., Deeney, M., Pastorino, S., Miller, M.R., Shah, A., Leon, D.A., Dangour, A.D., Green, R., 2022. Nitrate and nitrite contamination in drinking water and cancer risk: a systematic review with meta-analysis. Environ. Res. 210, 112988.

Pizarro, A.H., Torija, I., Monsalvo, V.M., 2018. Enhancement of pd-based catalysts for the removal of nitrite and nitrate from water. J. Water Supply Res Technol. 67, 615–625.
Pla-Tolós, J., Moliner-Martinez, Y., Molins-Legua, C., Campíns-Falcó, P., 2016. Colorimetic biosensing dispositive based on reagentless hybrid biocomposite: application to hydrogen peroxide determination. Sensors Actuators B Chem. 231, 837–846.
Radnia, H., Ghoreyshi, A.A., Younesi, H., Masomi, M., Pirzadeh, K., 2013. Adsorption of Fe(II) from aqueous phase by chitosan: application of physical models and artificial neural network for prediction of breakthrough. Int. J. Eng. Trans. B Appl. 26, 845–858.
Real Decreto 3/2023, of January 10, which establishes the technical-sanitary criteria for the quality of drinking water, its control and supply. Ministerio de la Presidencia, relaciones con las Cortes y memoria democrática, Gobierno de España. BOE-A-2023-628.
Robles-Jimarez, H.R., Jornet-Martínez, N., Campíns-Falcó, P., 2023. New green and sustainable tool for assessing nitrite and nitrate amounts in a variety of environmental waters. Water 15, 945.
Sanjuán, I., Montiel, V., Solla-Gullón, J., Expósito, E., 2019. Procedimiento para la reducción electroquímica de nitratos en agua mediante combinaciones de Bi y Sn. Patents ES-2713374B2, ES-2713374A1, WO2020128121A1.
Sanjuán, I., García-Cruz, L., Solla-Gullón, J., Expósito, E., Montiel, V., 2020. BiSn nanoparticles for electrochemical denitrification: activity and selectivity towards N_2 formation. Electrochim. Acta 340, 135914.
Santafe-Moros, A., Gozalvez-Zafrilla, J.M., Lora-García, J., 2005. Performance of commercial nanofiltration membranes in the removal of nitrate ions. Desalination 185, 281–287.
Sharma, S., Bhattacharya, A., 2017. Drinking water contamination and treatment techniques. Appl Water Sci 7, 1043–1106.
Steffen, W., Richardson, K., Rockström, J., Cornell, S.E., Fetzer, I., Bennett, E.M., Biggs, R., Carpenter, S.R., Vries, W. de, Wit, C.A. de, Folke, C., Gerten, D., Heinke, J., Mace, G.M., Persson, L.M., Ramanathan, V., Reyers, B., Sörlin, S., 2015. Planetary boundaries: guiding human development on a changing planet. Science 347, 1259855.
Tokazhanov, G., Ramazanova, E., Hamid, S., Bae, S., Lee, W., 2020. Advances in the catalytic reduction of nitrate by metallic catalysts for high efficiency and N2 selectivity: a review. Chem. Eng. J. 384, 123252.
Vaish, B., Srivastava, V., Singh, P.K., Singh, P., Singh, R.P., 2019. Energy and nutrient recovery from agro-wastes: rethinking their potential possibilities. Environ. Eng. Res. 25, 623–637.
Vinod, P.N., Chandramouli, M.K., 2015. Estimation of nitrate leaching in groundwater in an agriculturally used area in the state Karnataka. India, using existing model and GIS, Aquatic Procedia 4, 1047–1053.
World Health Organisation (WHO), 2011. Guidelines for Drinking-water Quality, 4th ed, ISBN 978-92-4-154995-0 (Geneva).
World Health Organization (WHO), 2003. Nitrate and Nitrite in Drinking-water. Background Document for Development of WHO Guidelines for Drinking-water Quality.
Xiao, H.-F., Shao, D.-D., Wu, Z.-L., Peng, W.-B., Akram, A., Wang, Z.-Y., Zheng, L.-J., Xing, W., Sun, S.-P., 2020. Zero liquid discharge hybrid membrane process for separation and recovery of ions with equivalent and similar molecular weights. Desalination 482, 114387.